Sawtooth oscillations directly driven by solar wind dynamic pressure enhancements

D.-Y. Lee

Department of Astronomy and Space Science, College of Natural Sciences and Institute for Basic Science Research, Chungbuk National University, Cheongju, Chungbuk, South Korea

L. R. Lyons

Department of Atmospheric Sciences, University of California, Los Angeles, California, USA

K. Yumoto

Space Environment Research Center, Kyushu University, Fukuoka, Japan

Received 24 September 2003; revised 30 December 2003; accepted 22 January 2004; published 2 April 2004.

[1] We have examined four well-defined events of sawtooth oscillations in energetic particle flux and magnetic field at geosynchronous orbit. During all four events, nearly simultaneous energetic particle flux enhancements and magnetic field variations occurred at all MLTs for each sawtooth cycle. Geomagnetic H component data at low to middle latitude also show a global H increase simultaneously with the geosynchronous responses at all MLTs, and the northern and southern PC indices generally show increases at each sawtooth cycle. All these are what is expected if solar wind pressure enhancements impacted the magnetosphere at times appropriate to have caused the onset of each sawtooth cycle. By directly checking the solar wind data, we find that there indeed exists a series of solar wind dynamic pressure enhancements for each sawtooth event. In identifying these pressure enhancements, we have found that the relative change in the dynamic pressure is important, particularly when the magnitude of the dynamic pressure is small and that even a modest dynamic pressure enhancement can result in significant changes in the magnetosphere when the IMF stays strongly southward for a long interval. We show that each cycle of the sawtooth oscillation can be reasonably associated in timing with a corresponding solar wind dynamic pressure enhancement. On the basis of this association and the global, simultaneous geosynchronous and ground responses, we suggest that the sawtooth oscillations studied in this paper are directly driven by series of solar wind pressure enhancements and are not a repetitive internal magnetospheric response to sustained enhanced solar wind energy input. *INDEX TERMS:* 2784 Magnetospheric Physics: Solar wind/magnetosphere interactions; 2778 Magnetospheric Physics: Ring current; 2788 Magnetospheric Physics: Storms and substorms; 2730 Magnetospheric Physics: Magnetosphere—inner; *KEYWORDS:* storm, sawtooth oscillation, energetic particle injection, substorm, solar wind dynamic pressure

Citation: Lee, D.-Y., L. R. Lyons, and K. Yumoto (2004), Sawtooth oscillations directly driven by solar wind dynamic pressure enhancements, *J. Geophys. Res.*, *109*, A04202, doi:10.1029/2003JA010246.

1. Introduction

[2] Successively occurring enhancements in energetic particle fluxes and concurrent magnetic field changes are often observed at geosynchronous orbit during intervals of sustained southward IMF (Interplanetary Magnetic Field), such as geomagnetic storms and steady magnetospheric convection periods. These changes have become known as sawtooth oscillations, and they are currently a key issue in storm-substorm related research. *Reeves et al.* [2004] examined a sawtooth event on 4 October 2000 and suggested that the sawtooth oscillations were a sequence of storm-time substorms, which, together with the quasi-steady convection electric field, contribute to the storm development. *Huang* [2002] and *Huang et al.* [2003] studied several sawtooth events. They also suggested that sawtooth oscillations were a sequence of substorms and suggested that they had an intrinsic occurrence periodicity of 2–3 hours. They further argued that the impact of a solar wind pressure enhancement could trigger the onset of sawtooth oscillations, but, following the initial pressure impact, the remaining cycles of the sawtooth oscillations were determined by the intrinsic nature of the periodic occurrence of substorms. While it was argued in the above studies that the sawtooth particle enhancements were due to substorms, sawtooth particle enhancement occur nearly simultaneously over more than 12 hours of MLT, in contrast to the far more

0148-0227/04/2003JA010246$09.00

limited range of nightside MLTs for which simultaneous energetic particle enhancements typically occur during substorms. Thus if the enhancements are due to substorms, the substorms must be of a far more global nature than ordinary substorms. In fact, *Reeves et al.* [2002] found on the basis of LANL particle data that the regions of sawtooth injections on 18 April 2002 were much wider in local time than the injection region of typical substorms. By using the ground magnetic data from midlatitude and low-latitude stations of the Circum-pan Pacific Magnetometer Network (CPMN) [*Yumoto*, 2001], *Kitamura et al.* [2002] found that the local-time distribution of the amplitude of the associated magnetic bay is consistent with the result of *Reeves et al.* [2002]. They also showed that Pi2 pulsations took place at the times of all sawtooth injections on 18 April 2002; they also showed that the local-time distribution of the orientations of the Pi2 pulsations was consistent with that of typical substorms [*Lester et al.*, 1984]. These results suggest that the sawtooth oscillations on 18 April 2002 corresponded to repeated substorms.

[3] In addition to substorms, abrupt enhancements in the solar wind dynamic pressure can cause significant magnetosphere-ionosphere disturbances. These are far more global in nature than are substorms in several aspects. The most well-known such disturbance is the sudden commencement of geomagnetic storms, which is generally due to the passage of an interplanetary shock ahead of a coronal mass ejection approaching the Earth. However, solar wind pressure pulses also exist at many other times, including during the main phase of storms and during convection bays. For example, a well-defined pulse in the solar wind pressure was observed during the main phase of the storm on 10 January 1997, resulting in a global enhancement in auroral activity and DP2 currents [*Shue and Kamide*, 1998; *Lyons et al.*, 2000; *Zesta et al.*, 2000], a disturbance which is far different from substorms. A similar global brightening of the aurora in response to a solar wind dynamic pressure enhancement was reported by *Chua et al.* [2001], who also reported other distinct differences between the pressure pulse driven auroral enhancement and that of typical substorms. The global nature of the magnetospheric response to changes in solar wind dynamic pressure has also been revealed in magnetic fields at geosynchronous orbit [e.g., *Rufenach et al.*, 1992; *Wing and Sibeck*, 1997; *Wing et al.*, 2002]. Additionally, enhancements in energetic particles have been observed to occur nearly simultaneously over a wide range of local times in response to solar wind dynamic pressure enhancements [*Li et al.*, 2003; *Lukianova*, 2003], in contrast to the more limited local time range for which such flux enhancements occur during substorms. *Boudouridis et al.* [2003] found that an increase (decrease) of auroral zone (polar cap) size and an increase in the total precipitating auroral particle energy flux is caused by the solar wind pressure enhancements, which is also a global reaction in contrast to the far more localized premidnight disturbance of substorms. In addition, *Lukianova* [2003] and *Boudouridis et al.* [2004] have found enhancements in polar cap convection, in contrast to the reductions that have been observed in association with substorms [*Lyons et al.*, 2003].

[4] Recently, we have found that solar wind pressure enhancements during southward IMF cause dipolarization-like changes of geosynchronous magnetic field on the nightside. These changes were found to occur nearly simultaneously with magnetic field compression on the dayside, with geosynchronous energetic particle enhancements observed on the nightside and dayside, and with global increases in the low-latitude H component of ground magnetic field. We thus argued that the solar wind pressure driven geosynchronous dipolarization is part of the global direct response to solar wind pressure enhancements, rather than part of the more localized response to a substorm [*Lee and Lyons*, 2004, hereinafter referred to as Paper 1].

[5] Motivated by the global nature of the sawtooth particle enhancements, we investigate in the present work the possibility that sawtooth oscillations are a response to successive solar wind dynamic pressure enhancements, rather than a result of repetitive substorms driven by a intrinsically internal magnetospheric processes as inferred by *Reeves et al.* [2004], *Huang* [2002], and *Huang et al.* [2003]. We have selected four events of sawtooth oscillations from geosynchronous spacecraft data and have examined them in comparison with solar wind data, low-latitude to midlatitude geomagnetic data, and the polar cap index. We find strong evidence that the sawtooth oscillations are directly driven by a series of solar wind dynamic pressure enhancements, suggesting that they are not successively occurring substorms. The paper is organized as follows. First, in section 2 we briefly describe the data and the methodology used here. In sections 3–6 we present four events of sawtooth oscillations in detail. Last, in section 7 our main results are summarized with some relevant discussion.

2. Data and Methodology

[6] We have examined the period 1998–2002 to find sawtooth events based on the criterion that LANL (Los Alamos National Laboratory) spacecraft proton flux enhancements (at 50–400 keV) have at least a few cycles in each event series. On the basis of preliminary statistical results, we have found that many sawtooth events are associated with not only solar wind pressure enhancements but also with near-simultaneous IMF changes. This makes the analysis difficult. In the present work we focus only on events for which the IMF Bz remained reasonably steadily southward, with no significant northward turnings that can trigger a substorm. Further, we consider only events for which low-latitude geomagnetic data are available from a sufficient number of stations covering a broad MLT range around the earth and for which both northern and southern PC index data are available. The above criteria are satisfied for sawtooth events that occurred during storm intervals on 17–18 April 2002, 20–21 August 2002, 25 September 1998, and 14 October 2000. Figure 1 shows the Dst values for those storms and the sawtooth intervals as indicated by horizontal arrows. The events began during the storm main phase and lasted until the early part of the storm recovery phase. For each of the sawtooth oscillation events, solar wind dynamic pressure and IMF conditions were examined using measurements by the Wind, ACE, and Geotail spacecraft. Geosynchronous magnetic fields from the GOES spacecraft, the geomagnetic H-component data from low-

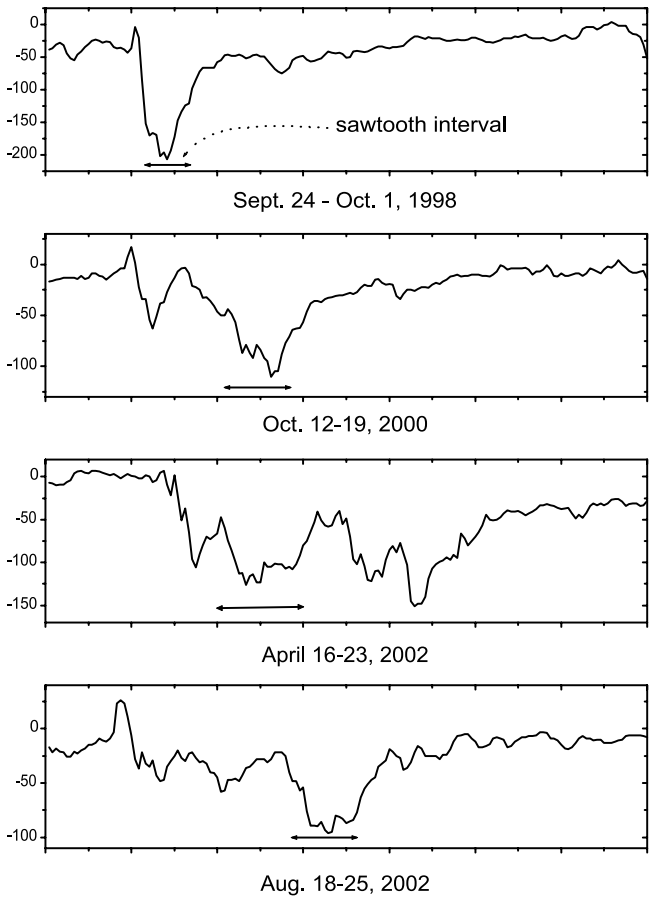

Figure 1. Dst corresponding to the four sawtooth events studied in this paper.

latitude to midlatitude ground stations and the PC index data were used to supplement the interpretation.

3. The 17–18 April 2002 Event

[7] Figure 2 shows the LANL energetic particle fluxes and the GOES geosynchronous magnetic fields. The first three panels show the proton fluxes within energy channels of 50–75 keV (uppermost curve) to 250–400 keV from three LANL spacecraft, and the next two panels display total magnetic field strength B, the z-component of magnetic field B_z, and the magnetic elevation angle θ from GOES 8 and 10. The time intervals when each spacecraft was located on the nightside (1800–0600 MLT) are indicated by horizontal arrows in each panel. Adjacent spacecraft are separated by ~2–4 hours in MLT so that these five spacecraft give good MLT coverage, covering ~12 hours in MLT.

[8] There are 10 proton flux variations, which are marked by vertical dotted lines and numbered in sequence from 1 to 10 in Figure 2. The average period of these sawtooth oscillations is ~2.6 hours. Variations 2–4 are the most well-defined, while variations 8 and 9 are somewhat more complex than the others. A common feature to these 10 variations is that most flux variations are preceded by gradual flux decreases, and the subsequent enhancements are nearly simultaneous at all energy channels (some enhancements are not seen in the 50–75 keV channel owing to high background in this channel). The electrons also show very similar flux oscillations, though the data is not shown here. The magnetic field variations are large for variations 1–5 when both GOES spacecraft were mostly on the nightside but much smaller for variations 6–10 when the GOES spacecraft were mostly on the dayside. This much weaker response for variations 6–10 might be due in part to smaller solar wind pressure enhancements for most of these events (as seen in Figure 3). It may also reflect an MLT dependence of the magnetic field response, as is most clearly seen for variation 4 where the variations are seen to be large at GOES 10 located about 1 hour prior to midnight but weak at GOES 8 located ~3 hr after midnight. On the nightside, the magnetic field change associated with the sawtooth flux enhancements look similar to the dipolarizations that occur during substorms. Notice the pattern that B_z and θ increase and the total field magnitude B decreases seen by both GOES 8 and GOES 10. It should be also mentioned that these B_z increases, in this and in subsequent events, are sometimes preceded by weak decreases in B_z such as in variation 2 seen by GOES 8 and variation 5 seen by both GOES 8 and 10. Such decrease has been interpreted as a response to an increase in the cross-tail currents [e.g., *Rufenach et al.*, 1992; *Wing and Sibeck*, 1997; *Wing et al.*, 2002].

[9] It is important to note that each of the 10 variations occurred nearly simultaneously at spacecraft at different MLTs. (Throughout this paper, nearly simultaneous implies within ~5 min. We do not consider ~5 min or less differences as a function of MLT, as have been reported at geosynchronous orbit in response to solar wind pressure changes in a study not confined to storm time events [*Wing et al.*, 2002], since such differences are well below those that are typical of the substorm dispersed geosynchronous response.) Furthermore, there are great similarities in structure between different curves of the data from different spacecraft. Variations 2–4 most clearly demonstrate all these features, for which both proton flux and magnetic field variations are large and well-defined. Variation 3 was observed to have occurred nearly simultaneously at five spacecraft at different MLTs: LANL 1991–080 at 18.4 MLT, LANL 1994-084 at 15.4 MLT, LANL-97A at 12.2 MLT, GOES 8 at 0.4 MLT, and GOES 10 at 20.4 MLT. Variation 2 consists of two or more peaks that appear similarly in both the LANL proton flux data and the GOES magnetic field data. Also, notice the double peak structure in variation 3, which is most clearly seen in the curves of the LANL-97A proton flux near noon and the GOES 8 magnetic field near midnight. The near-simultaneous occurrence of the variations at all MLTs and the great similarity in the structure of the curves from the different spacecraft data are what is expected from a global magnetospheric response to solar wind dynamic pressure variations.

[10] In order to demonstrate this possibility, we present the solar wind data in Figure 3, which shows the IMF from ACE spacecraft and the solar wind dynamic pressure from ACE and Wind. For reference, selected LANL proton flux data are also shown. Figure 3a indicates that during this sawtooth interval, the IMF B_z was strongly southward, ~−5 to −14 nT, without any clear variations. *Kitamura et al.* [2003] also looked at this 17–18 April 2002 event and

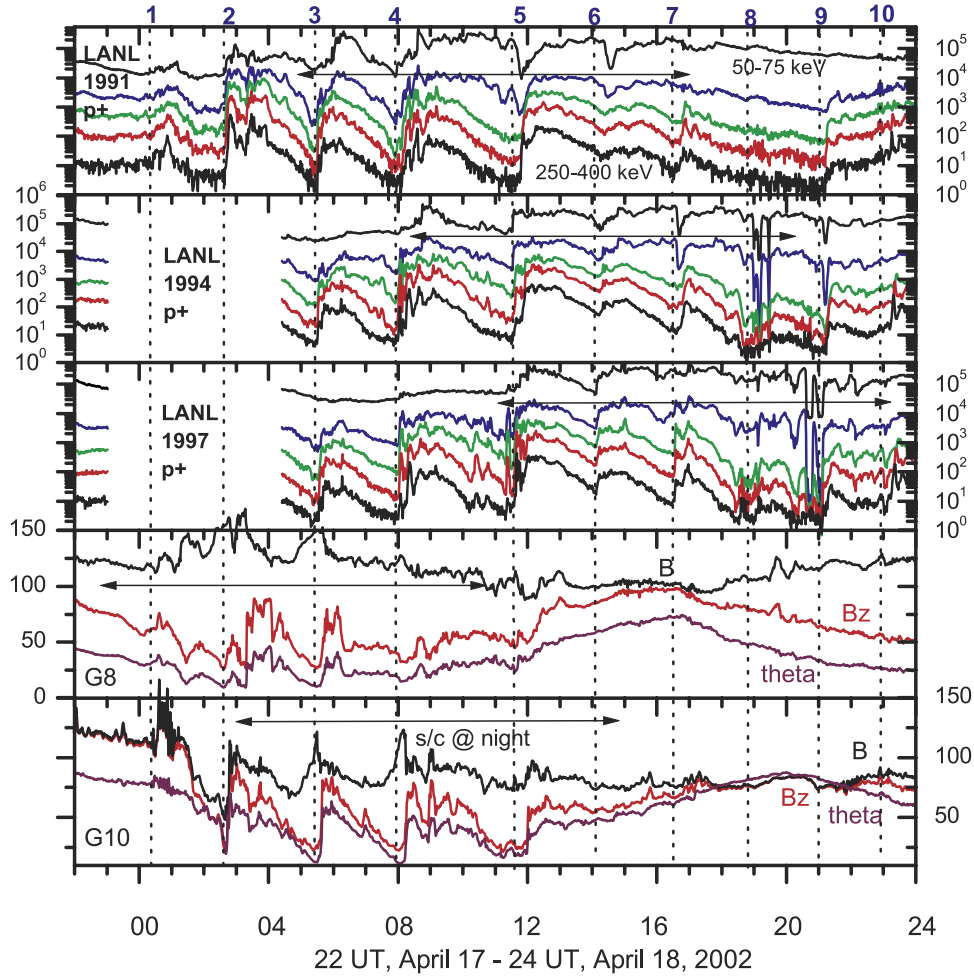

Figure 2. Data of the energetic proton flux (LANL spacecraft) and geosynchronous magnetic field (GOES) on 17–18 April 2002.

compared ground magnetic field data observed at CPMN stations, including data shown in Figure 4 of this paper, with the IMF B_z measured by the ACE satellite. They identified six magnetic bays during this sawtooth event, and found that for five of the six bays there was no clear simultaneous IMF-B_z variation. (The only exception was the variation 6 of this paper, at 1310 UT on 18 April at ACE.) Figure 3b displays the dynamic pressure data from ACE and shows a series of enhancements in dynamic pressure (Note that a log scale is used to identify the dynamic pressure enhancements more clearly). Those enhancements that can reasonably be associated with the 10 energetic particle flux enhancements are numbered in sequence from 1 to 10 in Figure 3b. The time delays for this association were not chosen to be identical for each flux enhancement. In particular, for variations 7 and 8, they are somewhat longer than the others. Such significant variation in the time delays can reasonably be expected, since large variations are known to occur in the orientation of solar wind structures [e.g., *Riazantseva et al.*, 2003]. However, the time delays we have taken are all of the order of 1 hour, which represents a typical transit time from ACE to the magnetosphere. While it is not possible to tell if we have identified each pressure enhancement correctly, it is remarkable that a pressure enhancement seen by ACE can be associated in terms of timing with each of the 10 sawtooth variations, as marked by dotted red lines for visual comparison. This consistency in timing between sawtooth variations and solar wind pressure variations provides direct evidence for our suggestion that the present sawtooth oscillation is directly driven by the sequence of solar wind pressure enhancements.

[11] We notice from Figure 3b that not all of these pressure enhancements at ACE appear as sharp changes. Some enhancements are rather modest, and there are a few cases for which we could not precisely make associations between solar wind pressure enhancements and LANL particle flux and/or GOES B_z enhancements (e.g., the pressure enhancement observed by ACE at 1900 UT and the B_z-increase seen by GOES 8 between 0100 and 0200 UT). Figures 3e and 3f show the solar wind dynamic pressure from Wind (in linear and log scales, respectively, for the reason discussed below), located $y = \sim 200\ R_E$ duskward from the Sun-Earth line. It can be seen that the dynamic pressure seen at Wind had quite different temporal structure than that seen by ACE. For example, the pressure decrease seen by ACE prior to the pressure increase labeled 1 was not detected at Wind, and the pressure enhancements seen by ACE after the first 2–3 large enhancements are

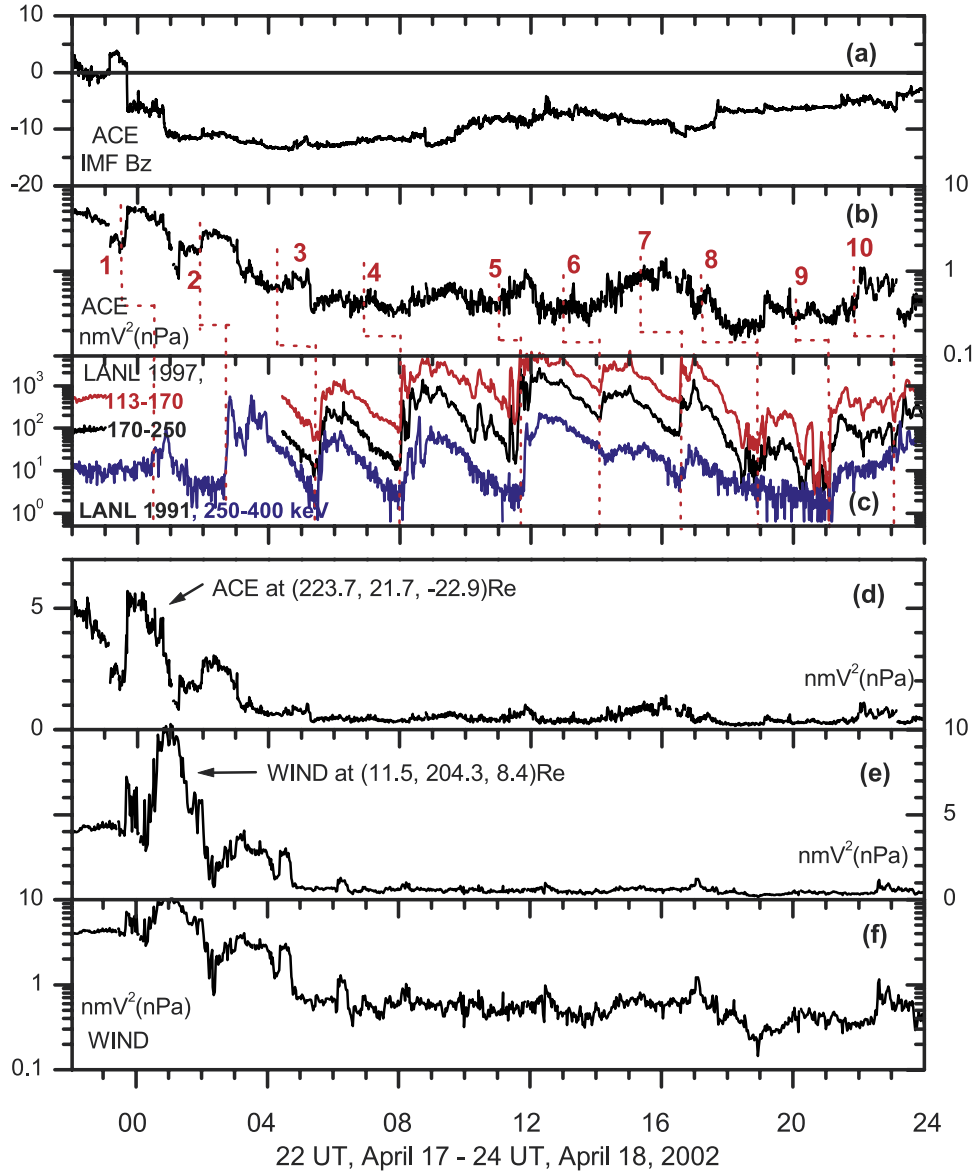

Figure 3. Data of the IMF (ACE) and solar wind dynamic pressure (ACE, Wind) on 17–18 April 2002. LANL proton flux data are also shown for selected channels for reference.

much less obvious at Wind. This implies significant spatial inhomogeneity in the solar wind and demonstrates the necessity of relying on spacecraft measurements in the vicinity of the Sun-Earth line to most reliably determine the solar wind structure that actually interacts with the magnetosphere. It must be remembered that ACE was located ~32 R_E off the Earth-Sun line so that some of the dynamic pressure variations observed at ACE may not precisely represent that which actually impacted the magnetosphere. It demonstrates why a precise one-to-one association between solar wind pressure enhancements seen by ACE and the geosynchronous responses could not be done for a few cases in this event. Another possible reason is that there could have occurred near-simultaneous substorm effects on the nightside due to small reductions in southward IMF. Nevertheless, the correspondence between the solar wind pressure enhancements and the geosynchronous responses is quite significant overall and is further verified using the geomagnetic H component and PC index data below (see Figure 4).

[12] In Paper 1, we found that relatively modest (~0.5 nPa) enhancements in solar wind dynamic pressure can cause significant enhancements in energetic particle fluxes when the IMF is strongly southward and the solar wind dynamic pressure is low (below ~1 nPa). This is clearly seen in Figure 3 and appears to be generally the case in the sawtooth events we have analyzed. For example, variation 4 of the sawtooth oscillation is quite significant in the proton flux change even though the corresponding observed solar wind enhancement was from ~0.3 nPa to ~0.6 nPa. This pressure increase also resulted in significant changes in the geosynchronous magnetic field at GOES 10 although the change is much weaker at GOES 8 due to a possible MLT effect [*Wing et al.*, 2002]. Below, we verify that this modest pressure increase significantly affected the magnetosphere by noting that a significant geomagnetic

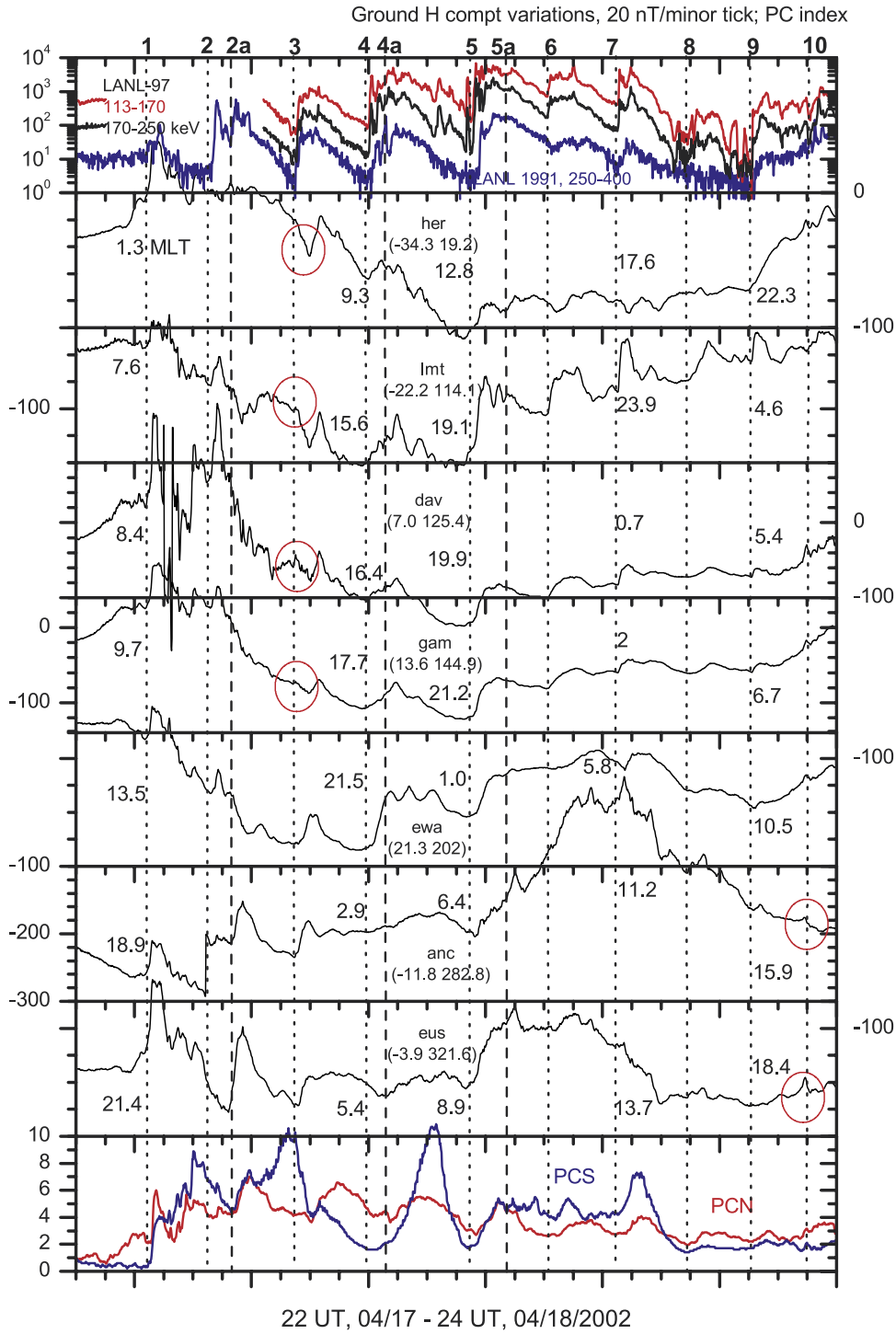

Figure 4. Geomagnetic H-component data from seven low-latitude to midlatitude stations and PC indices together with geosynchronous energetic particle data at selected channels for comparison for the 17–18 April 2002 event.

H-component increase occurred at low to middle latitude at nearly all MLTs.

[13] While the enhancement in the solar wind pressure was modest in magnitude for many of the sawtooth particle enhancements, the increases are significant when compared with the total dynamic pressure. For example, the pressure increase associated with variation in 4 in Figure 3 is a factor of ~2. That pressure enhancements such as number 4 caused a significant magnetospheric response suggests that it is necessary to identify significant relative changes in dynamic pressure, and not just those that are large in absolute magnitude. To identify such changes when the solar wind pressure varied considerably during the course of a sawtooth event, we plotted dynamic pressure on a log scale, as in Figure 3b and 3f. This was helpful in clearly identifying changes in the relative magnitude of dynamic

pressure. Figures 3d and 3e show the ACE and Wind data using the normal linear scale. From these plots, only the first two pressure enhancements appear clearly, and it is difficult to tell if there were any further enhancements. In fact, the recent work on this same event, *Huang* [2002] used a linear plot and did not note the presence of the series of solar wind pressure enhancements except for the first one. This suggests that one should be very careful when identifying solar wind pressure enhancements, remembering that the relative enhancement in pressure can be quite important, even if the absolute magnitude of the enhancement is modest.

[14] In the previous paragraph we have tried to associate an observed enhancement of dynamic pressure with each of the 10 sawtooth flux enhancements, as shown in Figure 3. Further verification can be done by using other data to determine whether a pressure enhancement actually impacted the magnetosphere at the time of the respective particle flux enhancement. The geomagnetic variation data from low-latitude to midlatitude stations and the PC index are helpful for this purpose. For the present event, we present the geomagnetic H-component data from seven selected low-latitude to midlatitude stations that give good coverage of nearly all MLTs and the southern and northern hemisphere PC index as shown in Figure 4. The MLT values of the geomagnetic stations are indicated for selected times in Figure 4, and energetic proton flux data at selected energies from LANL 1991-080 and LANL-97A are also shown for reference. The 10 major, as well as additional three subsidiary, sawtooth variations are indicated by vertical lines. Figure 4 shows that for most sawtooth flux increases, geomagnetic H-component increases occurred at nearly all MLT stations and that they are observed nearly simultaneously with each other and with the flux increases. This is what is expected from the enhancement in magnetopause current that occurs in response to solar wind pressure enhancements. We notice that H-variations at some MLTs exhibit decreases (red circles). This is most prominent for variation 3 at MLTs from late morning to the afternoon. We suspect that this is due to the strong response of other current systems to solar wind pressure enhancements. For example, the H-decrease on the afternoon side may be from partial ring current enhancement [*Shi et al.*, 2003], and the decrease seen at the two highest latitude stations (HER and LAQ (LAQ data not shown as this is very similar to that at HER)) could be due to dayside field aligned currents [*Zesta et al.*, 2000]. Note that enhancement of the partial ring current, which generally peaks earthward of geosynchronous orbit, could also help contribute to the observed enhancement of the geosynchronous B_z. Thus the response of geomagnetic H reinforces our interpretation that the sawtooth flux increases are due to the sequence of solar wind pressure enhancements.

[15] The PC index is a measure of convection on open polar cap fields, poleward of the ionospheric conductivity variations resulting from auroral precipitation (see *Lukianova et al.* [2002] and references therein for discussion of the southern and northern hemisphere PC indices, their differences and similarities, and their correlation with the strength of polar-cap convection). During periods of steady IMF, increases in the PC index reflect increases in polar cap convection that result from increases in solar wind dynamic pressure, as described by *Lukianova* [2003]. As can be seen in Figure 4, there were significant increases in the PC indices for most of the 10 primary sawtooth flux enhancements as well as at the times of the subsidiary flux enhancements labeled as 2a and 4a in Figure 4. This association is not perfect; however, the association of the PC index increases with the flux enhancements can be seen to be approximately as good as is the association of the enhancements in one of the PC indices with those in the other. Thus the association with the flux increases is as good as can be expected from such a single station index.

[16] The combination of the PC index response and the low-latitude/midlatitude ground magnetic response, together with the ACE dynamic pressure observations, gives strong support to the possibility that significant solar wind dynamic pressure enhancements impacted the magnetosphere at the times of each sawtooth flux enhancements and were thus primarily responsible for the enhancements. The IMF Bz was not completely steady during the entire sawtooth event. It is possible that there were small reductions in southward IMF associated with some of the individual flux enhancements so that some substorm effects could simultaneously have occurred on the nightside. However, the global nature of the geosynchronous flux enhancements and magnetic field effects and the simultaneous enhancements in the low-latitude/midlatitude ground H component and the PC indices suggest that the solar pressure effect was the dominant cause of the sawtooth oscillations.

4. The 20–21 August 2002 Event

[17] Figure 5 shows the geosynchronous data from four LANL and two GOES spacecraft for this sawtooth event in the same format as in Figure 2. These six spacecraft together cover a quite wide MLTs range, ~18.5 hours. Six major variations are identified, four of which are multiple, as marked by vertical dotted lines and numbered in sequence. The average period of this sawtooth oscillation is ~3.2 hours. All major proton flux variations are nearly dispersionless in energy. On the nightside the magnetic field variations appear as dipolarizations, while dayside fields are simply compressed. As seen before in Figure 2, the B_z increases in some dipolarizations are preceded by weak decreases in B_z, for example, variation 6 seen by GOES 10. All the variations of magnetic field and proton flux for each sawtooth cycle are nearly simultaneous at all MLTs. Again this is what is expected if the sawtooth oscillations are a direct response to a series of solar wind pressure enhancements.

[18] To demonstrate the existence of solar wind pressure enhancements, the corresponding solar wind and IMF data are presented in Figure 6. The IMF data from Geotail are shown in the top panel, the solar wind dynamic pressure data from ACE and Geotail are presented in the next two panels, and selected LANL proton flux data and the GOES magnetic field elevation angle data are shown in the last two panels for reference. The locations of these solar wind spacecraft are indicated in GSE coordinates in each corresponding panel. Again, the IMF is strongly southward for this sawtooth interval, although there were some northward turnings that lead to reduced southward IMF. The difference in dynamic pressure between the two spacecraft again implies the existence of spatial inhomogeneities in the solar wind. The Geotail location is much closer to the

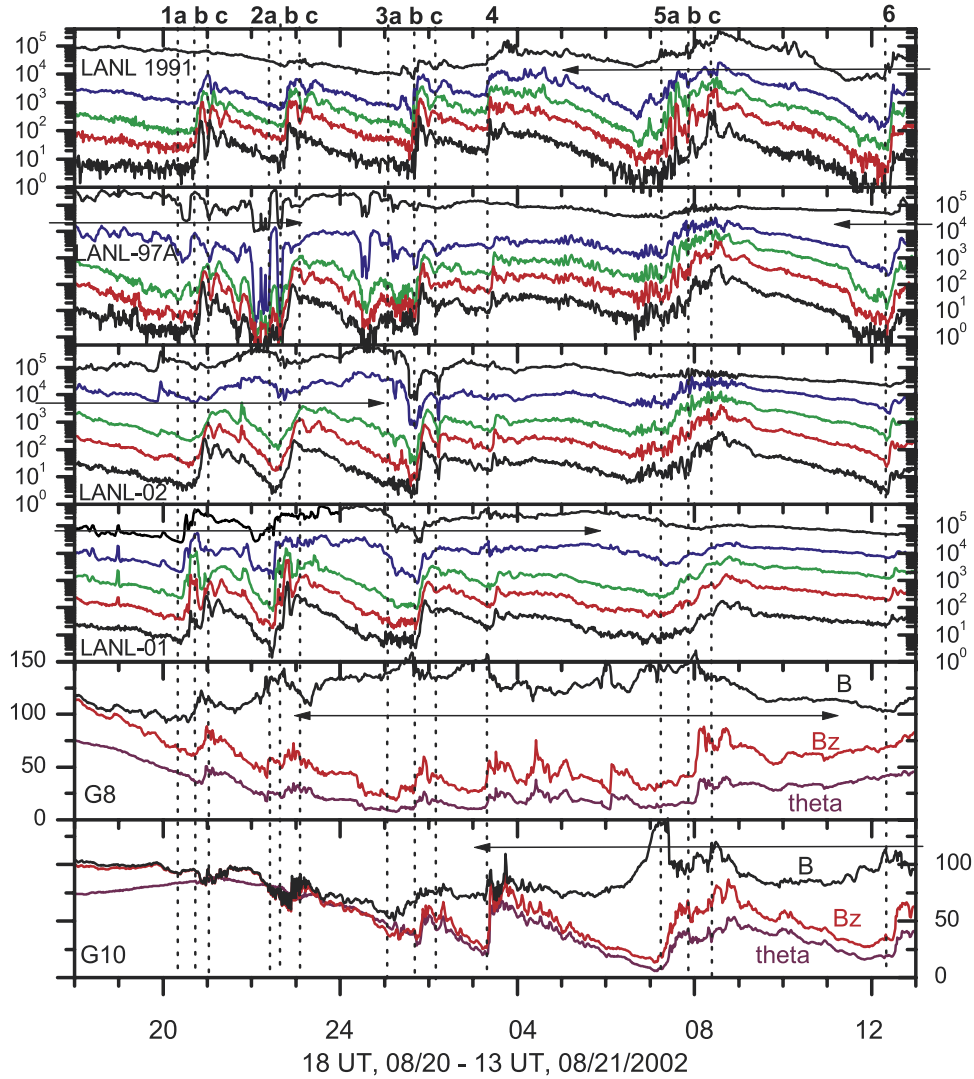

Figure 5. Data of the the energetic proton flux (LANL spacecraft) and geosynchronous magnetic field (GOES) on 20–21 August 2002.

Sun-Earth line, $y = \sim 8.7\ R_E$ to 16.5 R_E, than ACE. Pressure enhancements associated with each of the sawtooth flux enhancements can clearly be identified in the Geotail observation, as identified by the sequentially numbered dotted lines in Figure 6c. Furthermore, pressure enhancements can be seen separately for each of the observed multiple flux enhancements, demonstrating excellent correspondence between the solar wind pressure enhancements and the sawtooth particle flux enhancements. We notice that details of solar wind pressure variations, such as their multipeak structure, are seen in the sawtooth variations. For example, notice the multiple peak structure that appear very similarly both in the Geotail solar wind pressure and the GOES magnetic field during the intervals indicated by horizontal red-color arrows in Figures 6c and 6e. For a few of our associations in Figure 6, the solar wind lag times are somewhat longer than the others, suggesting that the pressure changes for these events were oriented at relatively large angles to the Earth-sun line. The impacts of solar wind pressure increases are verified by the global and near-simultaneous enhancements of the geosynchronous proton flux and the geomagnetic H-component, and the near-simultaneous increases of the PC index as discussed below. Therefore we conclude that this sawtooth event is also most likely due to the sequence of solar wind pressure enhancements.

[19] The ACE measurement, taken $\sim 43\ R_E$ off the Earth-Sun line, saw most of the major enhancements, but not all the multiple enhancements could be discerned nor could an enhancement for event 4. Wind (observations not shown) saw even less of the pressure enhancements, presumably because it was located at $y = \sim 79\ R_E$. These observations demonstrate the necessity of being aware of solar wind structure in the plane perpendicular to the Earth-Sun line. It we were to have used the ACE observations alone, the association of the sawtooth flux enhancements with the solar wind enhancements would have been suggestive but not very definitive. If we had relied on the Wind observations, we probably would not have noted an association. Only with Geotail is there a good, almost one-to-one, correspondence in timing between each of the solar wind enhancements and each enhancement of the sawtooth oscillations. In addition, the pressure enhancements are more prominent in magnitude at Geotail than at ACE and Wind.

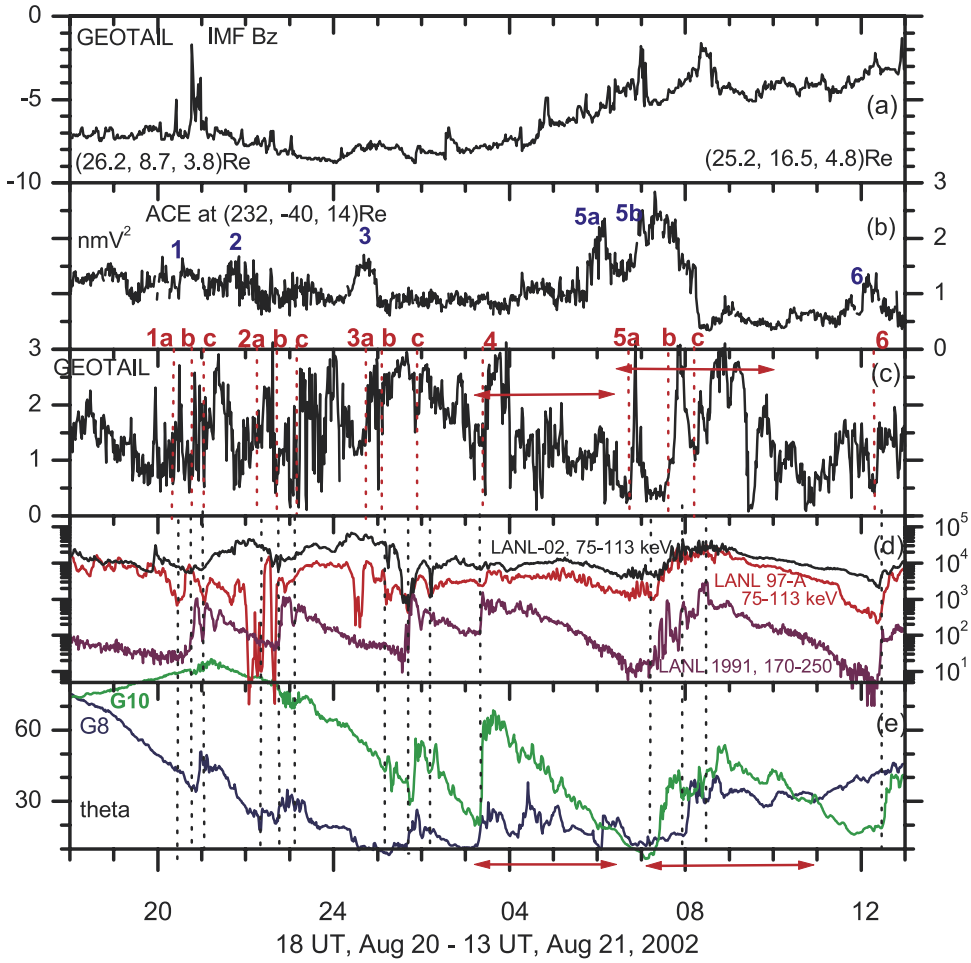

Figure 6. Data of the IMF (Geotail) and solar wind dynamic pressure (ACE, Wind, Geotail) together with LANL proton flux and GOES magnetic field on 20–21 August 2002.

[20] Again, the geomagnetic H-component data from low-latitude to midlatitude stations and the PC indices are helpful for evaluating this event. The H-component data are presented in Figure 7. For reference, the GOES magnetic elevation angle data are shown in the top panel. H-component increases can be seen at most MLT stations in association with all the sawtooth variations. Even the multiple enhancements can often be seen in the H-component data. Furthermore, it is interesting to note that the multipeak structure found in the Geotail solar wind pressure and GOES 8 magnetic field for variation 4 is also seen in the H-component variation as indicated by arrows, most prominently at DAV, ANC and EUS, which were located near noon or near midnight. The PC indices also show increases for each sawtooth flux enhancement, and also show some association with the multiple flux increases, as seen in Figure 7. Therefore the geomagnetic H-component and PC index responses give support to the idea that solar wind pressure enhancements caused the particle flux enhancements during this sawtooth interval.

5. The 25 September 1998 Event

[21] Figure 8 shows the geosynchronous energetic proton flux data from three LANL spacecraft, the geosynchronous magnetic field data from GOES 8 spacecraft, and the PC indices in the same format as before. Here we are interested in the six major and two subsidiary variations as marked by vertical lines and numbered in sequence. The average period of the major oscillations is ~1.9 hours. The proton flux changes show well-defined dropouts and enhancements at all MLTs. The magnetic field variations look more complex but appear as dipolarizations on the nightside and as compressions on the dayside. As seen before in Figure 2 and Figure 5, the B_z increases in some dipolarizations are preceded by small decreases in B_z, for example, variations 1 and 3 seen by GOES 8. Also, an MLT dependence is seen for variations 4–6, in that the geosynchronous magnetic response on the morningside is weak while the proton flux variations on the duskside are significant. We again notice nearly simultaneous occurrences of these variations at all MLTs for each sawtooth cycle.

[22] To demonstrate the solar wind conditions for this sawtooth event, we show the IMF from ACE and the solar wind dynamic pressure from ACE, Wind, and Geotail in Figure 9. For Geotail, the number density (red line) is shown together with the dynamic pressure to fill in data gaps that occur when the solar wind velocity, and thus the dynamic pressure, is not available. The LANL proton data are also shown for selected energy channels in the bottom panel. The locations of these solar wind spacecraft near 0600 UT are indicated in GSE coordinates in each

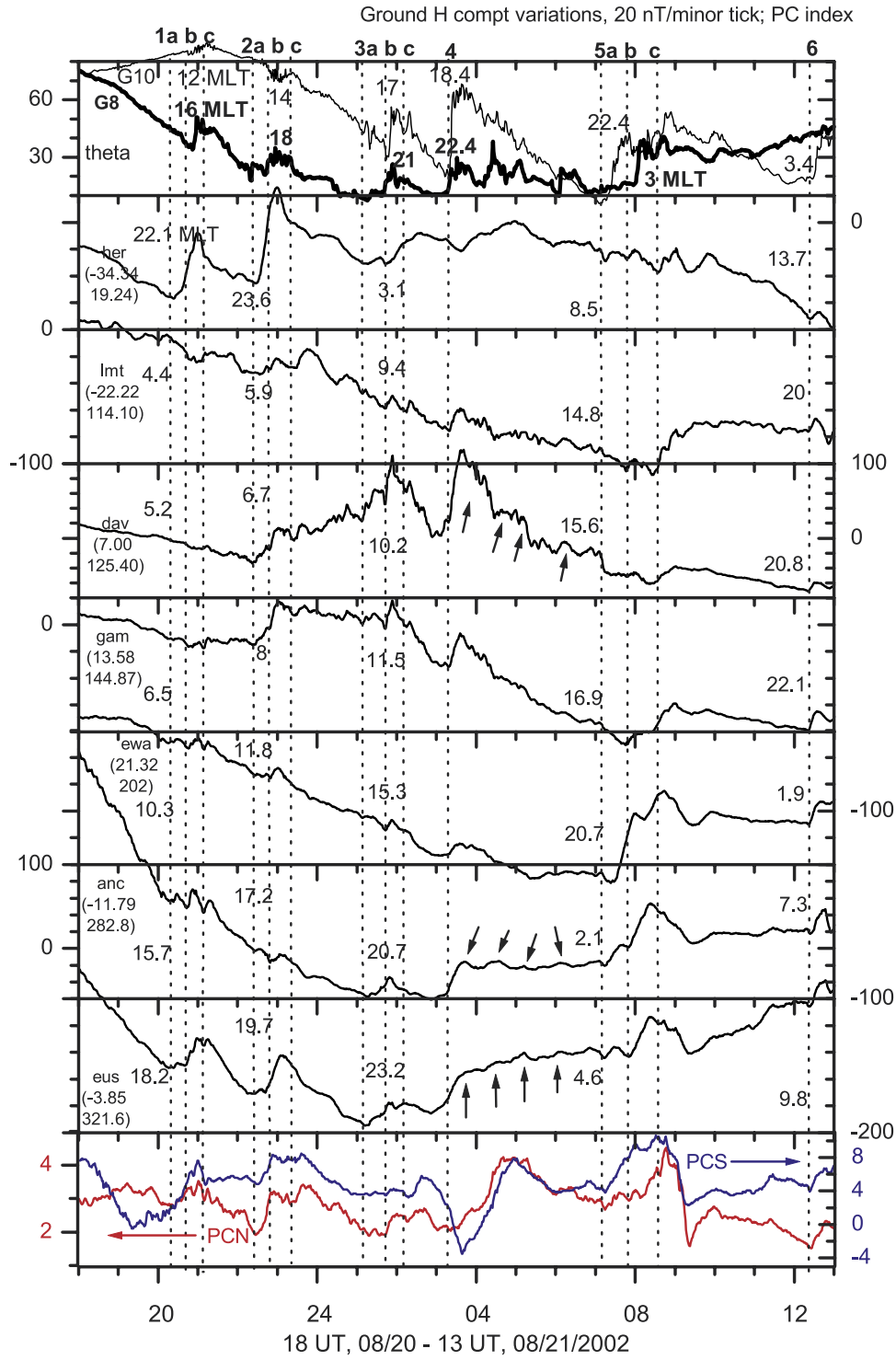

Figure 7. Geomagnetic H-component data from seven low-latitude to midlatitude stations and PC indices together with geosynchronous magnetic field elevation angle data for comparison for the 20–21 August 2002 event.

corresponding panel. It is seen that the IMF has long intervals of strongly southward B_z component which also exhibits northward turning at several instants. For this event, there is overall consistency in the dynamic pressure data between three spacecraft measurements. The dynamic pressure exhibits a series of enhancements in all three spacecraft measurements as marked by vertical dotted lines and the corresponding sequence of numbers. The six major and two subsidiary variations in the sawtooth are also marked by the vertical dotted lines in the bottom panel. It is seen that there is excellent one-to-one correspondence in timing between the solar wind pressure enhancements and

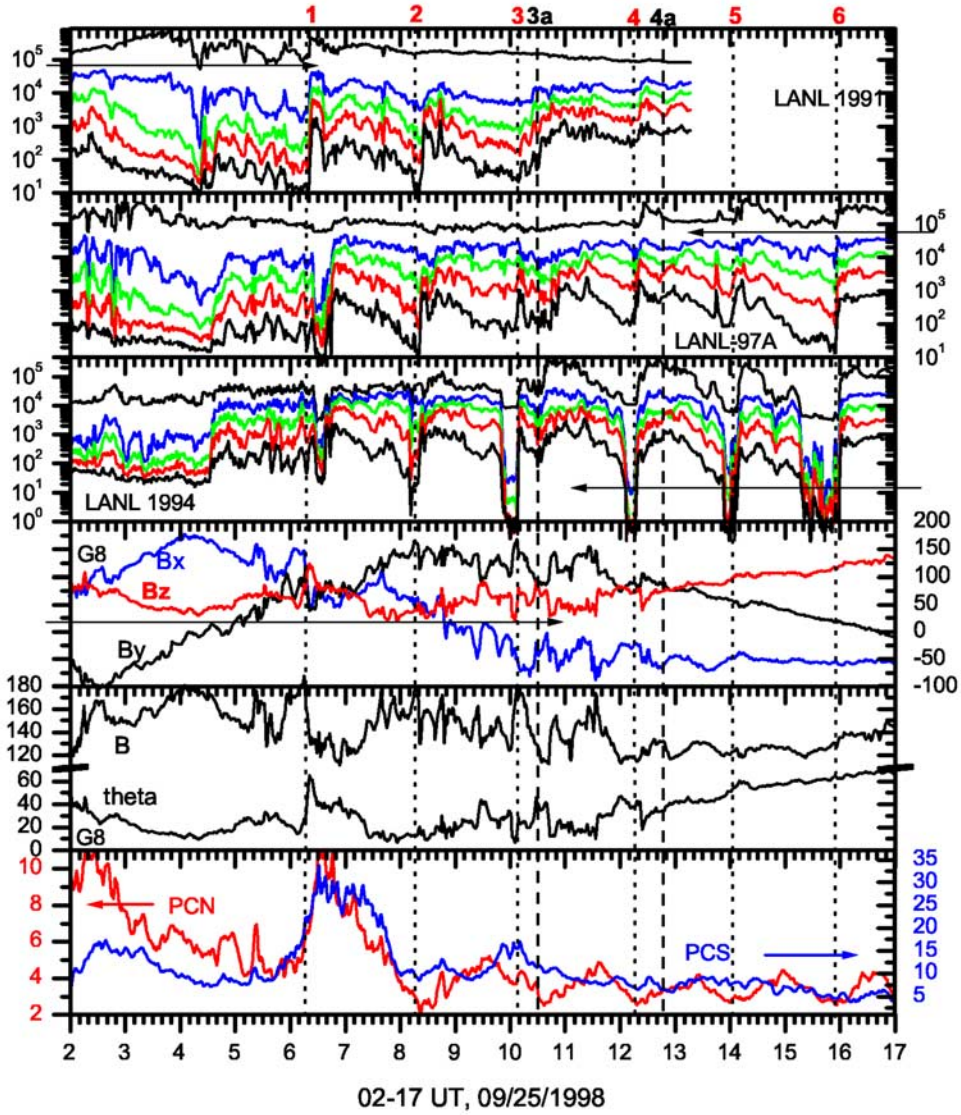

Figure 8. Data of LANL proton flux, GOES 8 magnetic field, and PC indices on 25 September 1998.

the sawtooth flux enhancements. There are two evident pressure enhancements that we have not associated with a sawtooth flux enhancement, one initiating at ~1110 UT at Geotail, which can also be seen at Wind and ACE, and one initiating at 1435 UT at Geotail, which can also be seen at ACE. These enhancements can be seen to correspond to geosynchronous particle flux enhancements that were not large enough to be identified as a sawtooth enhancement.

[23] Also, we have checked low-latitude to midlatitude geomagnetic H-component data for this sawtooth intervals (data not shown here). As for the earlier two events, nearly simultaneous global H-increase appeared at most MLT stations. As before, there are few exceptions when an H-decrease is seen due to stronger effect from other current systems. Also the PC indices show quite good associations with each sawtooth enhancement as can been seen in Figure 8. We thus conclude that this sawtooth oscillation is quite consistent with being driven by the sequence of solar wind pressure enhancements.

[24] This event is one of the three events that were already examined recently by *Huang et al.* [2003]. However, they noted only the first pulse, number 1, near 0600 UT in the Wind data, but did not mention the subsequent solar wind enhancements. In fact they even state that the solar wind pressure stabilized after the first pulse. However, as with the 18 April 2002 event, the average dynamic pressure for this event varied considerably during the course of the event. To demonstrate how this may lead to the discrepancy between their interpretation and ours, we plot the solar wind dynamic pressure from Wind in both linear and log scales in Figure 10. Clearly, from the normal linear plot, as used by *Huang et al.* [2003], it is difficult to recognize the existence of the pressure enhancements after the first two biggest pulses, while it is far easier to do so from the log scale plot. We stress that one should not simply ignore the pressure change when the absolute magnitude of the pressure appears to be small because what appears to be more important is the relative change in the dynamic pressure rather than the absolute value. Also, as mentioned earlier, relatively modest

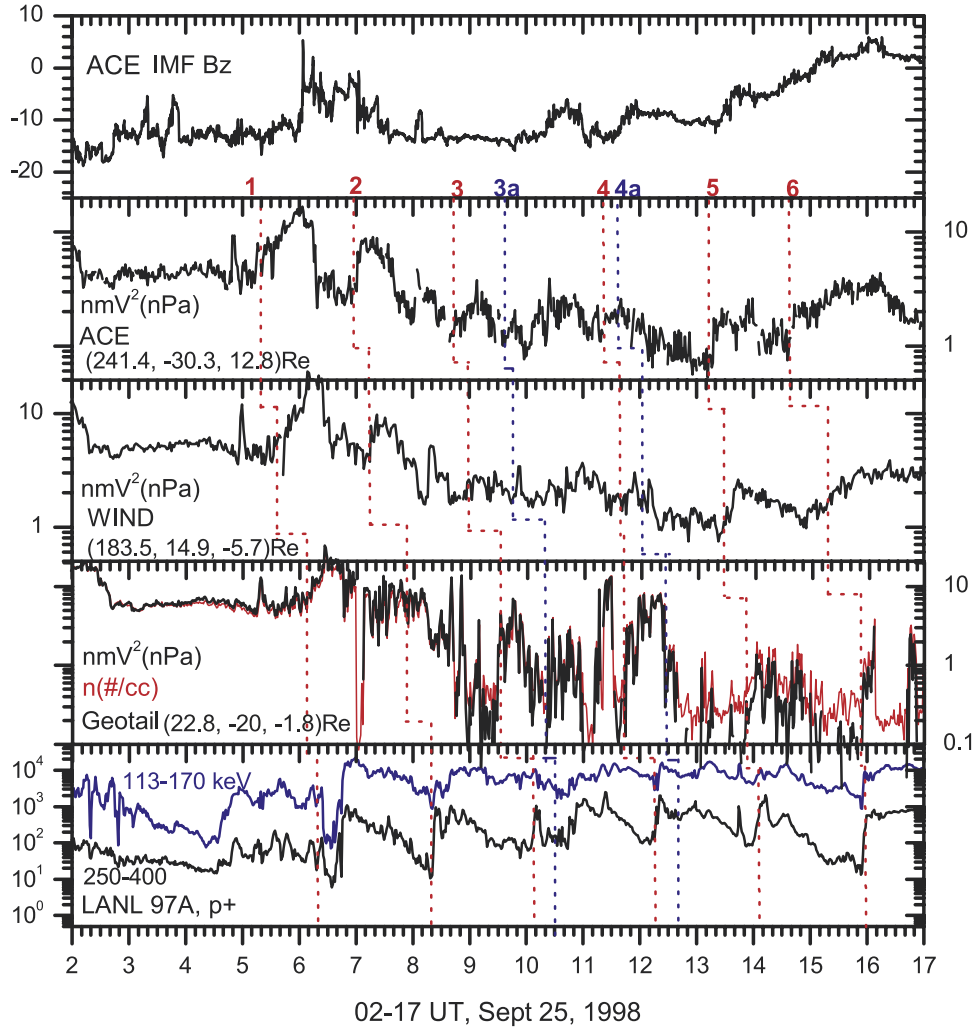

Figure 9. Data of IMF (ACE) and solar wind dynamic pressure (ACE, Wind, Geotail) together with LANL data on 25 September 1998. The Geotail data also show the particle number density in red-colored line.

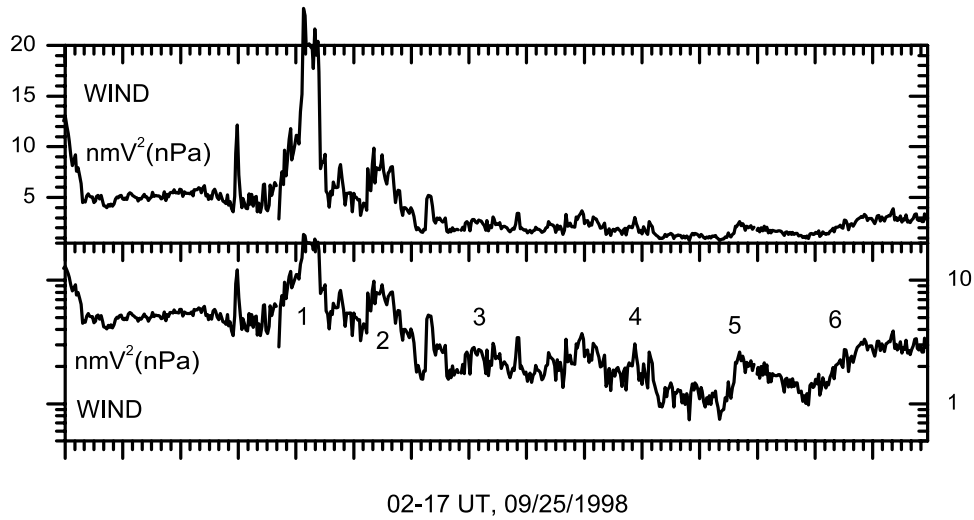

Figure 10. Linear and log scale plots of the solar wind dynamic pressure from Wind for the 25 September 1998 event.

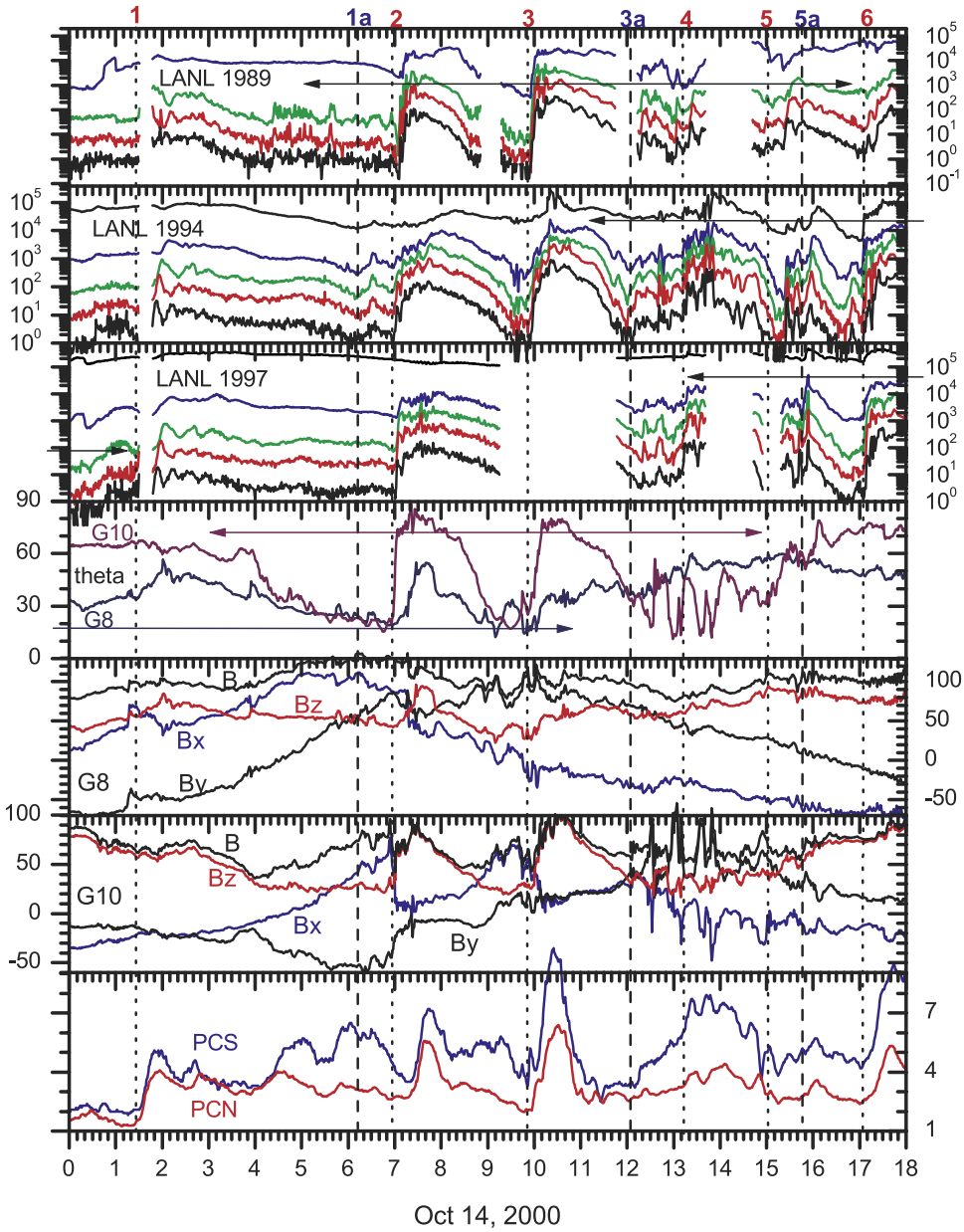

Figure 11. Data of LANL proton flux, GOES magnetic field, and PC indices on 14 October 2000.

enhancements can result in significant changes in the magnetosphere under strongly southward IMF, as in the present event.

6. The 14 October 2000 Event

[25] The geosynchronous proton data from three LANL spacecraft and the magnetic field data from GOES 8 and 10 for this event are shown in Figure 11, along with the PC indices, in the same format as before. A total of six major and three subsidiary variations are of interest here as marked by vertical lines and numbered in sequence. The average period of this sawtooth oscillation excluding the rather remote first one is ~2.5 hours. Again the proton flux changes exhibit well-defined enhancements, mostly being preceded by dropouts. Some of the nightside magnetic variations look like magnetic dipolarizations, most notably for variations 2 and 3. The MLT dependence is also seen as the geosynchronous magnetic response is larger at GOES 10 than at GOES 8. More importantly, we see simultaneous occurrences at quite wide MLTs for each sawtooth variation. For example, for the variation 2, the MLT locations of the five spacecraft near 0700 UT were ~20 MLT for LANL 1989-046, ~13.9 MLT for LANL 1994-084, ~11.7 MLT, ~02 MLT for GOES 8, and ~22 MLT for GOES 10, respectively. All changes in proton flux and magnetic field for this cycle can be seen to have occurred nearly simultaneously, implying the effect of a solar wind pressure enhancement.

[26] Association of this sawtooth event with solar wind conditions can be seen in Figure 12, which displays the IMF

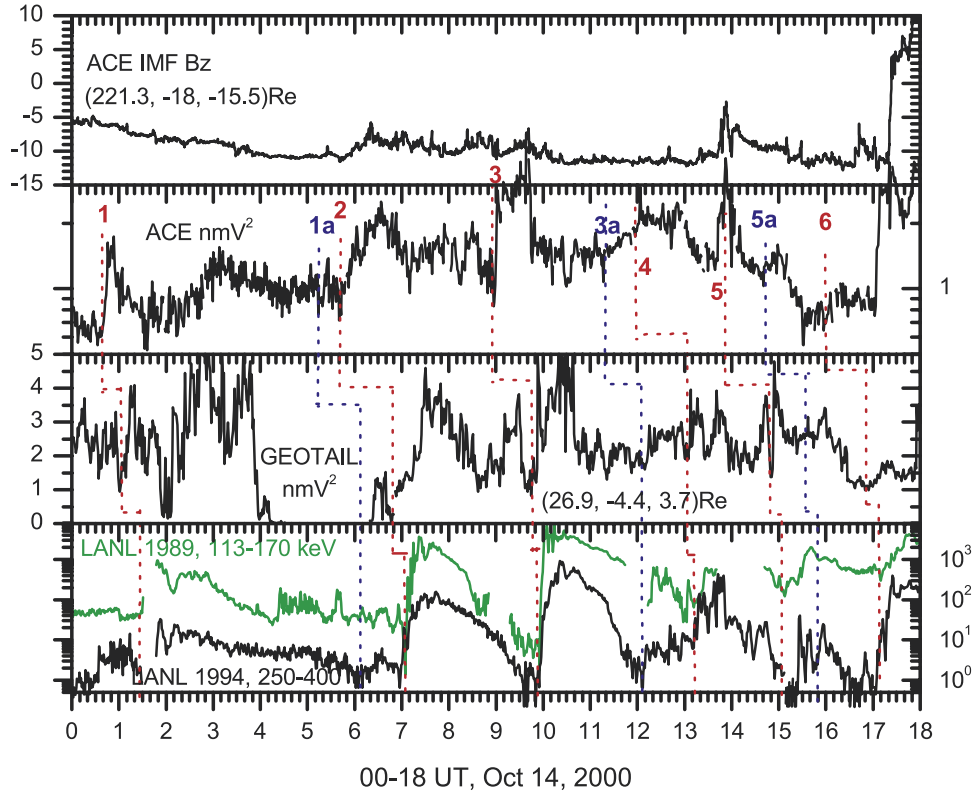

Figure 12. Data of the IMF (ACE) and solar wind dynamic pressure (ACE, Wind, Geotail) together with LANL data on 14 October 2000.

and solar wind dynamic pressure data from ACE and Geotail in the same format as before. For reference, LANL proton flux data for selected channels are also shown in the bottom panel. From the top panel, it is seen that the IMF was strongly southward for an extended period. A series of solar wind pressure enhancements are seen in both the ACE and Geotail data, as marked by successive numbers. There is quite good overall consistency between the ACE and Geotail measurements for this event, since the spacecraft were relatively close together in the yz-plane and both relatively near the Earth-Sun line. As indicated by vertical lines, there is good alignment between each sawtooth cycle and solar wind pressure enhancements. In fact, visual comparison of the Geotail and ACE data curves with the LANL proton flux data curves shows remarkable similarities between the profiles implying that the sawtooth variations are the direct response of the magnetosphere to the solar wind pressure enhancements. Also, as for the earlier events, the geomagnetic H-component data from low-latitude to midlatitude stations (data not shown) exhibit H-increases at most MLTs, and the PC indices generally show increases at the appropriate times as shown in Figure 11. This lends strong support for impacts of solar wind pressure enhancements being responsible for the global responses of the magnetosphere for this event.

7. Summary and Discussion

[27] In this paper we have presented four sawtooth events that were selected from well-defined storm periods to demonstrate their relationship with solar wind conditions. The sawtooth oscillations were identified from geosynchronous spacecraft measurements of energetic proton flux and magnetic field, which were then compared with the solar wind condition measured by ACE, Wind, and Geotail. The geomagnetic H-component data from low-latitude to midlatitude stations and the northern and southern PC indices were used to complement the interpretation. Average periods for these sawtooth oscillations are ~2.6, 3.2, 1.9, and 2.5 hours, respectively, giving a mean period of ~2.6 hours when averaged over all four events.

[28] We have shown that for each cycle of a given sawtooth oscillation, the variations at geosynchronous orbit as well as in the geomagnetic H-component were nearly simultaneous at different MLTs. Also, we have found that each series of sawtooth oscillations is well associated in timing with solar wind dynamic pressure enhancements that occur in series. The geomagnetic H-component data and the PC indices provide excellent verification that solar wind pressure increases impacted the magnetosphere at times appropriate to cause the global sawtooth oscillations. On the basis of these findings, we suggest that the sawtooth oscillations studied here were all global direct responses to sequences of solar wind dynamic pressure enhancements, and are not the result of an internal magnetospheric process that gives series of semiperiodic substorms.

[29] We have also found that identifying the existence of geoeffective solar wind pressure enhancements requires careful examination due to solar wind structure, particularly when the magnitude of the dynamic pressure is small. We

suggest that what may be more important is the relative change in the dynamic pressure rather than the absolute magnitude of the change. Also, even a relatively modest enhancement in the dynamic pressure can result in significant changes in the magnetosphere when the IMF stays strongly southward for a long interval. We have seen such sensitivity of the magnetosphere in Paper 1 and in the event in April 2002, for example.

[30] Two of our sawtooth events examined here, the April 2002 and September 1998 events, were recently studied by *Huang* [2002] and *Huang et al.* [2003]. Including these, they examined four sawtooth events. They concluded that of their four events only one was correlated with continuous solar wind pressure oscillations and for the other three no pressure oscillations were found after an initial large pressure pulse. On the basis of this, they argued that the impact of the initial solar wind pulse triggered the onset of these sawtooth oscillations but that the remaining cycles of the sawtooth oscillation were periodically occurring substorms due to some internal process within the magnetosphere. Further, they suggested that if continuous solar wind pressure enhancements are to be responsible for sawtooth oscillations, it is possible only when the period of such continuous pressure enhancements is coincidentally same as that of typical substorm cycle. On the other hand, we suggest that they have overlooked the existence of the series of pressure enhancements after the initial pulse as well as the global nature of the solar wind pressure effect, and our new interpretation instead suggests external driving of the entire cycle of the sawtooth oscillations by series of solar pressure enhancements.

[31] Many sawtooth events exist in addition to the four events studied here that we have inferred are directly driven by a series of solar wind pressure enhancements. In practice, it may be often difficult to directly identify the responsible solar wind pressure enhancements because the solar wind condition that actually interacts the magnetosphere may not be properly monitored by available spacecraft due to strong spatial inhomogeneities in the solar wind. However, the impact of solar wind pressure can still be verified in terms of global simultaneous occurrences of the geosynchronous particle flux and magnetic field changes, the low latitude H-component increases at all MLTs, and the PC indices increases. We have initiated a study using a larger database, and preliminary results show more sawtooth events that are in close correlation with continuous solar wind pressure enhancements. However, many individual sawtooth cycles are also associated with IMF variations such as a northward turning simultaneous with solar pressure enhancements. This implies that in reality many sawtooth events driven by solar wind pressure enhancements may be affected by IMF driven substorm effects to some extent. We thus encourage further studies of this in the future.

[32] **Acknowledgments.** We thank M. F. Thomsen, G. D. Reeves, J. E. Borovsky, M. G. Henderson, and C.-S. Huang for in depth discussions of sawtooth events and for their encouragement despite their differences in interpretation. We also thank E. Zesta, A. Boudouridis, C. P. Wang, China Lee, and E. S. Lee for their help with this work. This work was supported by grant R01-2002-000-00100-0(2002) from the Basic Research Program of the Korea Science and Engineering Foundation. This research was supported at UCLA in part by NSF grants OPP-0136139 and ATM-0207298. The energetic particle data used in this work were provided by G. D. Reeves through Los Alamos Energetic Particle home page of LANL geosynchronous spacecraft. The GOES magnetic field data were provided by H. Singer through NASA's cdaweb site. The solar wind plasma and magnetic field data of ACE, Wind, and Geotail used here were obtained from NASA's cdaweb site, and we are grateful to each of the principal investigators, D. J. McComas, N. Ness, K. Ogilvie, R. Lepping, L. Frank, and S. Kokubun. The geomagnetic data used for the April and August 2002 events were obtained from CPMN chain and the authors are grateful to K. Kitamura and the CPMN group for the help with the data. The northern hemisphere PC index was obtained from the web site of the World Data Center for Geomagnetism, Copenhagen, and we thank R. Lukianova for providing the southern PC index.

[33] Arthur Richmond thanks Renata Lukianova and Simon Wing for their assistance in evaluating this paper.

References

Boudouridis, A., et al. (2003), The effect of solar wind pressure pulses on the size and strength of the auroral oval, *J. Geophys. Res.*, *108*(A4), 8012, doi:10.1029/2002JA009373.

Boudouridis, A., E. Zesta, L. R. Lyons, P. C. Anderson, and D. Lummerzheim (2004), Magnetospheric reconnection driven by solar wind pressure fronts, *Ann. Geophys.*, in press.

Chua, D., G. Parks, M. Brittnacher, W. Peria, G. Germany, J. Spann, and C. Carlson (2001), Energy characteristics of auroral electron precipitation: A comparison of substorms and pressure pulse related auroral activity, *J. Geophys. Res.*, *106*, 5945.

Huang, C.-S. (2002), Evidence of periodic (2–3 hour) near-tail magnetic reconnection and plasmoid formation: Geotail observations, *Geophys. Res. Lett.*, *29*(24), 2189, doi:10.1029/2002GL016162.

Huang, C.-S., et al. (2003), Periodic magnetospheric substorms and their relationship with solar wind variations, *J. Geophys. Res.*, *108*(A11), 1255, doi:10.1029/2003JA009992.

Kitamura, K., H. Kawano, S. Ohtani, A. Yoshikawa, and K. Yumoto (2002), Local-time distribution of low-latitude ground magnetic disturbances at sawtooth injections of April 18–19, 2002, *Eos Trans. AGU*, *83*(47), Fall Meet. Suppl., F1120.

Kitamura, K., H. Kawano, S. Ohtani, A. Yoshikawa, K. Yumoto, and CPMN Group (2003), Quasi-periodic substorms during recovery phase of magnetic storm for space weather study, paper presented at the International Symposium on Information Sciences and Electrical Engineering 2003, Kyushu Univ., Fukuoka, Japan.

Lee, D.-Y., and L. R. Lyons (2004), Geosynchronous magnetic field response to solar wind dynamic pressure pulse, *J. Geophys. Res.*, *109*, A04201, doi:10.1029/2003JA010076.

Lester, M., W. J. Hughes, and H. J. Singer (1984), Longitudinal structure in PI-2 pulsations and the substorm current wedge, *J. Geophys. Res.*, *89*, 5489.

Li, X., et al. (2003), Energetic particle injections in the inner magnetosphere as a response to an interplanetary shock, *J. Atmos. Sol. Terr. Phys.*, *65*, 233.

Lukianova, R. (2003), Magnetospheric response to the solar wind dynamic pressure inferred from polar cap index, *J. Geophys. Res.*, *108*(A12), 1428, doi:10.1029/2002JA009790.

Lukianova, R., O. Troshichev, and G. Lu (2002), The polar cap magnetic activity indices in the southern (PCS) and northern (PCN) polar caps: Consistency and discrepancy, *Geophys. Res. Lett.*, *29*(18), 1879, doi:10.1029/2002GL015179.

Lyons, L. R., et al. (2000), Auroral disturbances during the January 10, 1997 magnetic storm, *Geophys. Res. Lett.*, *27*, 3237.

Lyons, L. R., S. Liu, J. M. Ruohoniemi, S. I. Solovyev, and J. C. Samson (2003), Observations of dayside convection reduction leading to substorm onset, *J. Geophys. Res.*, *108*(A3), 1119, doi:10.1029/2002JA009670.

Reeves, G. D., et al. (2002), "Global sawtooth activity" in the April 2002 geomagnetic storm, *Eos Trans. AGU*, *83*(47), Fall Meet. Suppl., F1113.

Reeves, G. D., et al. (2004), IMAGE, POLAR, and geosynchronous observations of substorms and ring current ion injection, in *Disturbances in Geospace: The Storm-Substorm Relationship*, *Geophys. Monogr. Ser.*, vol. 142, edited by A. S. Sharma et al., pp. 89–100, AGU, Washington, D. C.

Riazantseva, M. O., P. A. Dalin, G. N. Zastenker, and J. Richardson (2003), Orientation of sharp fronts of the solar wind plasma, *Cosmic Res.*, *41*(4), 382.

Rufenach, C. L., R. L. McPherron, and J. Schaper (1992), The quiet geomagnetic field at geosynchronous orbit and its dependence on solar wind dynamic pressure, *J. Geophys. Res.*, *97*(A1), 25.

Shi, Y., E. Zesta, and L. Lyons (2003), Effect of solar wind pressure enhancement on storm-time ring current asymmetry: Preliminary study, paper presented at Geospace Environment Modeling (GEM) workshop, Natl. Sci. Found. Div. of Atmos. Sci., Snowmass, Colo.

Shue, J.-H., and Y. Kamide (1998), Effects of the solar wind density on the westward electrojet, in *Substorms-4*, edited by S. Kokubun and Y. Kamide, p. 677, Kluwer Acad., Norwell, Mass.

Wing, S., and D. G. Sibeck (1997), Effects of interplanetary magnetic field z component and the solar wind dynamic pressure on the geosynchronous magnetic field, *J. Geophys. Res.*, *102*(A4), 7207.

Wing, S., D. G. Sibeck, M. Wiltberger, and H. Singer (2002), Geosynchronous magnetic field temporal response to solar wind and IMF variations, *J. Geophys. Res.*, *107*(A8), 1222, doi:10.1029/2001JA009156.

Yumoto, K. (2001), Characteristics of Pi 2 magnetic pulsations observed at the CPM N stations: A review of the STEP results, *Earth Planets Space*, *53*, 981.

Zesta, E., et al. (2000), The effect of the January 10, 1997, pressure pulses on the magnetosphere-ionosphere current system, in *Magnetospheric Current Systems*, *Geophys. Monogr. Ser.*, vol. 118, edited by S. Ohtani et al., p. 217, AGU, Washington, D. C.

D.-Y. Lee, Department of Astronomy and Space Science, College of Natural Sciences and Institute for Basic Science Research, Chungbuk National University, 48 Gaeshin-dong, Heungduk-gu, Cheongju, Chungbuk 361-763, South Korea. (dylee@ast.chungbuk.ac.kr)

L. R. Lyons, Department of Atmospheric Sciences, University of California, Los Angeles, 405 Hilgard Ave., Los Angeles, CA 90095-1565, USA. (larry@atmos.ucla.edu)

K. Yumoto, Space Environment Research Center, Kyushu University, 6-10-1 Hakozaki, Higashi-ku, Fukuoka 812-8581, Japan. (yumoto@serc.kyushu-u.ac.jp)